



Thermal and kinetics studies of primary, secondary and tertiary alkanolammonium salts of 4-nitrobenzoic acid

Manuela Crisan¹ · Gabriela Vlase² · Elisabeta I. Szerb¹ · Titus Vlase²

Received: 6 September 2017 / Accepted: 5 January 2018 / Published online: 23 January 2018
© Akadémiai Kiadó, Budapest, Hungary 2018

Abstract

Nitrobenzoic derivatives are chemically and biologically significant molecules, recently listed as active ingredients in the medical-pharmaceutical field. A series of *p*-nitrobenzoic acid salts were synthesized with different substituted alkanolamine (ethanolamine, diethanolamine and triethanolamine) via proton exchange reactions and characterized. Fourier transform infrared spectroscopy—FTIR-UATR, and a combination of thermal techniques (differential scanning calorimetry—DSC, and thermogravimetric analysis—TGA) with hot-stage microscopy were used in order to demonstrate the formation of salts and to analyse thermal stability and phase transitions. The aim of this study is to investigate thermal behaviour and kinetics of this class of compounds, previously poorly examined, which offers interesting phase transformations in the solid state. DSC indicated that the synthesized salts had very distinct melting points. Diethanolamine and triethanolamine used as cation in the formation of multicomponent systems with 4-nitrobenzoic acid lead to melting points near 100 °C, compared to compound based on ethanolamine. Calorimetric and thermogravimetric data indicate the absence of solvate forms in all studied compounds. TGA and kinetic experiments allowed the calculation of the activation energy, revealing that triethanolammonium salt has the highest stability in this studied series of compounds.

Keywords Alkanolammonium salts of 4-nitrobenzoic acid · Thermal stability · TG/DTG · DSC · Non-isothermal kinetics · Modified NPK method · Protic alkanolammonium ionic liquids (APILs)

Introduction

The interest in nitroaromatic compounds over the years as important structural elements for the synthesis of industrial chemicals, dyes, pigments or herbicides is well recognized [1–4]. These compounds, despite the potential toxicity issues [5, 6], have been known as therapeutics for Parkinson's disease, angina and insomnia [7–9], and recently their use in infectious diseases has been developed. Among these compounds, 4-nitrobenzoic acid has been listed as inhibitor agent for recognition of *Mycobacterium tuberculosis* complex and differentiation from non-

tuberculous mycobacteria [10, 11]. Considering the present and future prospects of nitro drugs based on the unique properties of nitro group and its ability to form hydrogen bonds, there is a compelling need for complex researches in this controversial topic.

In pharmaceutical industry, the salts represent about a half of all active pharmaceutical ingredients on the market, bringing an improvement in drug's physicochemical properties (e.g. melting point, chemical and physical stability, solubility, bioavailability and dissolution rate). In addition, selection of the appropriate anion/cation combination, keeping anion constant and changing the counterion or introduction of specific functional groups on the cation or anion can affect the physicochemical and biological properties of salt. An increasing number of 4-nitrobenzoate multicomponent complexes formed with organic cations such as aliphatic amines [12], guanidine [13, 14], 8-hydroxyquinoline [15], amino acids [16, 17], piperazine [18], pyridine [19], imidazole [20] are developed and studied

✉ Gabriela Vlase
gabriela.vlase@e-uvv.ro

¹ Institute of Chemistry Timisoara of Romanian Academy, 24 Mihai Viteazul Boulevard, Timisoara 300223, Romania

² Research Center: Thermal Analysis in Environmental Problems, West University of Timisoara, Pestalozzi Street 16, Timisoara 300115, Romania

recently in the literature as promising NLO materials or active pharmaceutical ingredients.

In the last years, searching for new compounds with potent biological activity and low toxicity seems to be a new trend in biosciences. Our previous studies highlighted the alkanolamines as promising molecules used as salt-forming agents and revealed the structural complexity and low toxicity of the system represented by alkanolamine salts with different aromatic carboxylic acids. These salts have provided interesting supramolecular networks with different topologies according to structural variation of counterions [21, 22], lower toxicity comparatively with aliphatic amines and heterocyclic amine salts [23] and biological activity in plants [24–26].

In this work we have focused on investigation of thermal behaviour and kinetics by thermal analysis techniques (DSC and TG/DTA) of alkanolammonium salts of 4-nitrobenzoate in order to highlight the nature of their solid state. Both counterions have active pharmaceutical properties and are economically, commercially available, which makes them promising for the design of new dual active compounds.

Materials and methods

All reagents, 4-nitrobenzoic acid—4-NBA, and the bases (ethanolamine—MEA, diethanolamine—DEA, triethanolamine—TEA) were purchased in analytical purity grade from Fluka AG (Buchs SG) and used as received.

The salts were prepared in a 1:1 molar ratio, dissolving the acid and the appropriate alkanolamine in acetone and then mixing the two solutions. The reaction was completed after 2 h of continuous stirring at room temperature, the salts precipitating in a crystalline state according to their solubility in acetone. The compounds were collected by filtration, washed with acetone and then dried in a vacuum for 3 h. The salts were recrystallized from acetone or ethanol. The suitable crystals for single-crystal X-ray diffraction analysis were obtained by slow evaporation at room temperature.

The purity of all studied salts was established via an UV spectrophotometric method, which consisted in determining the specific extinction (absorbance at λ_{\max} of a solution 1 g l^{-1} in a cell of 1 cm width) of the free acid (ϵ_a) and the corresponding salt (ϵ_s), by measuring the UV absorbance in NaOH 0.1 M at λ_{\max} .

$$\text{Purity} = \frac{\bar{\epsilon}_s \cdot M_s}{\bar{\epsilon}_a \cdot M_a} \cdot 100 \quad (1)$$

where M_s and M_a are the molecular weights for the salt and free acid, respectively.

FTIR spectra were performed using PerkinElmer Spectrum 100 FTIR spectrometer with UATR, in the range $4000\text{--}650 \text{ cm}^{-1}$ (see Fig. 1). Single-crystal X-ray diffraction analyses for all studied compounds were done at room temperature on a Xcalibur “Oxford Diffraction” diffractometer equipped with CCD area detector and a graphite monochromator utilizing $\text{MoK}\alpha$ radiation. Thermal behaviour was determined using a Diamond TG/DTA PerkinElmer in dynamic air atmosphere (synthetic air 5.0 Linde Gas with flow 100 mL min^{-1}). The experiments were carried out from $25 \text{ }^\circ\text{C}$ up to $500 \text{ }^\circ\text{C}$, at heating rates $\beta = 5, 7, 10, 12$ and $15 \text{ }^\circ\text{C min}^{-1}$, using open Al crucible (see Fig. 2). The phase transitions of the microcrystalline solids were observed using an Olympus BX53M polarizing microscope (POM) equipped with Linkam hot stage. Images of the various crystalline phases were recorded with an Olympus UC90 camera, using a filter with $\lambda = 530 \text{ nm}$. Differential scanning calorimetry study was performed with one PerkinElmer Diamond DSC using aluminium closed pans with heating and cooling rate of $10 \text{ }^\circ\text{C min}^{-1}$ in nitrogen 20 mL min^{-1} (5.0 Linde Gas).

Results and discussion

Synthesis and physicochemical characterization

A series of alkanolammonium salts of 4-nitrobenzoic acid were prepared according to “rule of three”, via proton exchange reaction, each base having a sufficiently high pKa to react with 4-nitrobenzoic acid (Table 1). In this principle, the degree of ionization is considered to be a critical parameter, the ΔpKa (pKa of base – pKa of acid) value being important for predicting salt or co-crystal formation. ΔpKa value greater than 3 leads to salt formation, while ΔpKa less than 0 lead to co-crystal formation [27].

The reaction has occurred rapidly, with high yields (90–92%). The compounds are water soluble and with well-defined melting points not exceeding ca. $0.5 \text{ }^\circ\text{C}$, which is an indicative of their high purity. All synthesized alkanolamine salts have showed lower melting points compared with 4-NBA. The values of purity determined by spectrophotometric method were between 99.12 and 99.36% (Table 2). UV spectroscopic data showed similar λ_{\max} values for salt and acid (4-NBA $\lambda_{\max} = 273.6 \text{ nm}$) that confirm the existence of the same anion in both compounds.

The evidence of proton transfer and molecular interactions between alkanolammonium cation and 4-nitrobenzoate anion is illustrated in the FTIR-UATR spectra (Fig. 1). The formation of salts was identified by: (a) the presence of asymmetric and symmetric $\nu_{(\text{COO}^-)}$ vibrations occurring at $1650\text{--}1540$ and $1450\text{--}1360 \text{ cm}^{-1}$, (b) N–H vibrations attributable to $-\text{NH}_3^+$, $-\text{NH}_2^+$ and $-\text{NH}^+$,

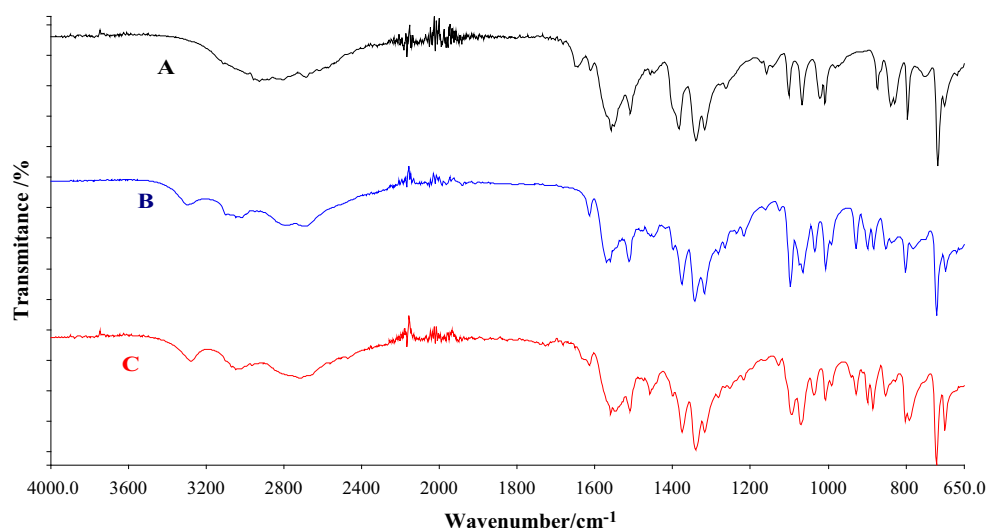


Fig. 1 FTIR-UATR of 4-nitrobenzoic acid salts prepared with ethanolamine (A), diethanolamine (B) and triethanolamine (C). A— $C_9H_{12}N_2O_5$ (228.20); FTIR-UATR ($1950 v_{max}/cm^{-1}$): 2930, 2689 ($-NH_3^+$), 1646, 1612, 1556, 1385 ($-COO^-$), 1102, 1068, 1021, 1009 (C—OH); B— $C_{11}H_{16}N_2O_6$ (272.26); FTIR-UATR ($1942 v_{max}/cm^{-1}$):

3031, 2738 ($-NH_2^+$), 1615, 1567, 1377 ($-COO^-$), 1098, 1066, 1035, 1007 (C—OH); C— $C_{13}H_{20}N_2O_7$ (316.31); FTIR-UATR ($1980 v_{max}/cm^{-1}$): 2722 ($-NH^+$), 1615, 1560, 1548, 1376 ($-COO^-$), 1095, 1071, 1037, 1008 (C—OH)

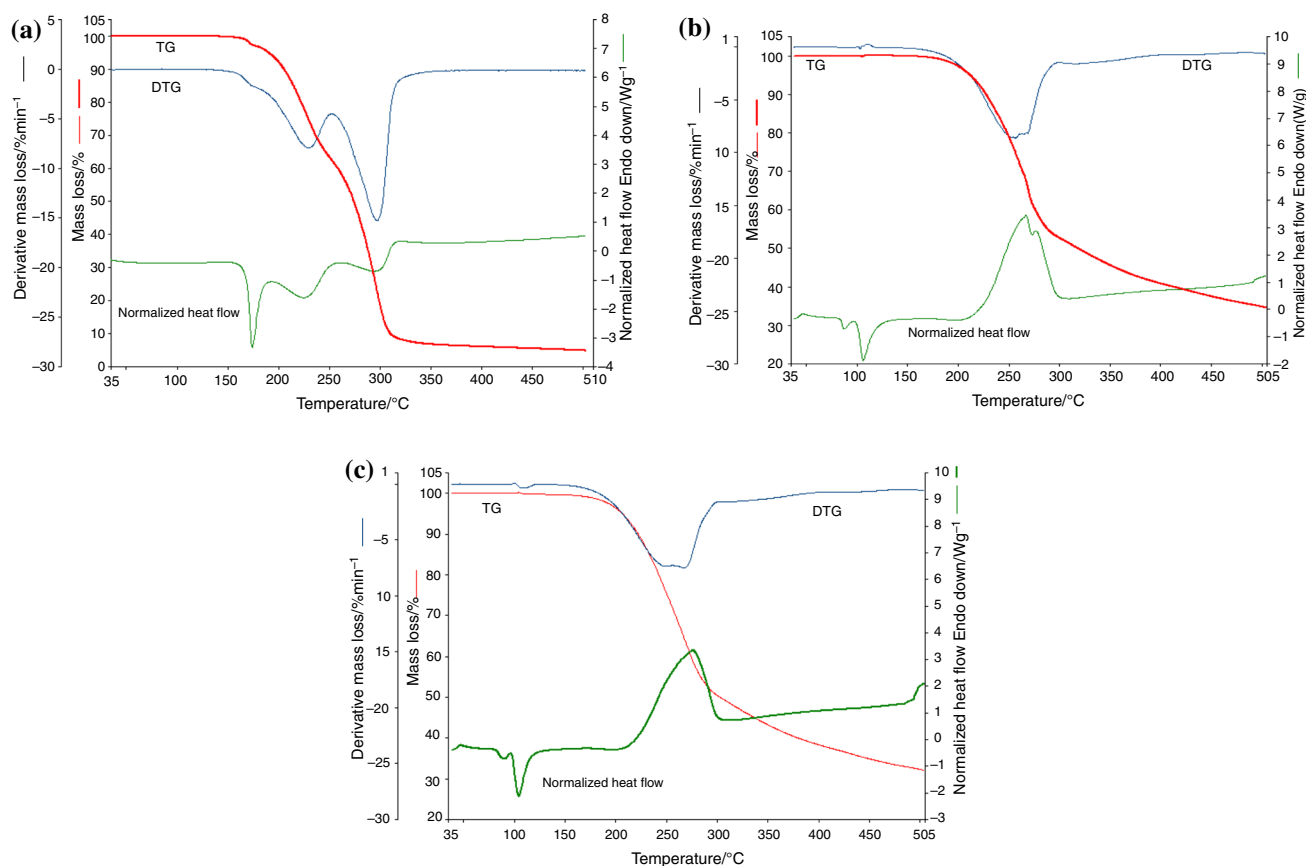
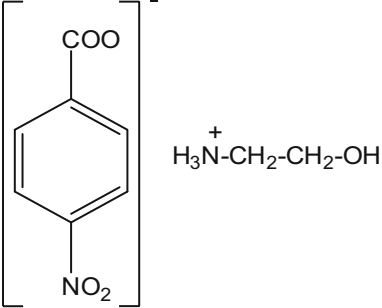
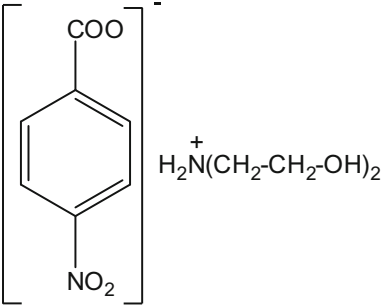
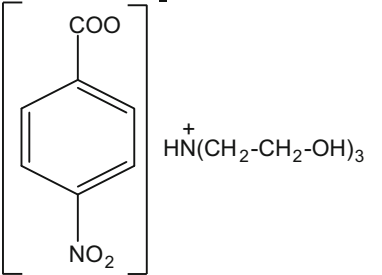


Fig. 2 TG/DTG/heat flow (in air) of 4-nitrobenzoic acid salts prepared with ethanolamine (a), diethanolamine (b) and triethanolamine (c) (in air at heating rates $\beta = 10 \text{ }^\circ\text{C min}^{-1}$)

stretching of solid ammonium salts $v_{NH_3^+} = 3200\text{--}2700 \text{ cm}^{-1}$, $v_{NH_2^+} = 3100\text{--}2700 \text{ cm}^{-1}$, $v_{NH^+} = 2800\text{--}2400 \text{ cm}^{-1}$ and

(c) the absence of stretching band $v_{C=O} = 1710\text{--}1680 \text{ cm}^{-1}$, characteristic for the carboxyl group [29, 30].

Table 1 Tabulated ΔpK_a of alkanolammonium salt/protic ionic liquid of 4-nitrobenzoic acid

No.	Compound name	Abbreviation	Structure	ΔpK_a^a
A	Monoethanolamine 4-nitrobenzoate	4-NBA MEA		6.06
B	Diethanolamine 4-nitrobenzoate	4-NBA DEA		5.52
C	Triethanolamine 4-nitrobenzoate	4-NBA TEA		4.32

^a $\Delta pK_a = pK_a(\text{base}) - pK_a(\text{acid})$ was calculated using pK_a data from PubChem Compound Database [28]. All pK_a values have been determined in aqueous solutions

Table 2 The purity values of studied compounds

Sample	$\lambda_{\text{max}}/\text{nm}$	Average specific extinction acid ϵ_a	Average specific extinction salt ϵ_s	Purity, $p/\%$
4-NBA MEA	273.6	58.42	42.45	99.22
4-NBA DEA	273.4		35.59	99.24
4-NBA TEA	273.4		30.67	99.36

The absorption bands reflected in FTIR-UATR spectra confirmed the conversion of carboxyl group of 4-NBA and amino group of alkanolamine into carboxylate and ammonium groups, indicating the complete proton transfer in studied compounds.

The crystallographic data of A–C compounds have revealed that the salt unit serves as building block for supramolecular architecture. The anions and cations are self-assembled via ionic $\text{N-H}\cdots\text{O}$ and normal $\text{O-H}\cdots\text{O}$ hydrogen bonds, compound A showing stronger intermolecular interactions [21], which leads to a higher

melting point compared to compounds B and C. Therefore, the force of attraction between the molecules affects the melting point of a compound.

Thermogravimetric analysis of compounds A–C

The TG/DTG/DTA curves of studied compounds recorded in air at a heating rate of $10\text{ }^\circ\text{C min}^{-1}$, and thermoanalytical data are presented in Fig. 2 and Tables 3 and 4, respectively. The thermoanalytical data obtained at 5 heating rates, $\beta = 5, 7, 10, 12$ and $15\text{ }^\circ\text{C min}^{-1}$ were used

Table 3 TG data of compounds A–C

Compound	Process	$T_{\text{onset}}/^\circ\text{C}$	$T_{\text{end}}/^\circ\text{C}$	$\Delta m/\%$
A	a	189.7	229.75	55.4
	b	229.75	274.9	39.24
B	a	202.2	288.7	50.6
C	a	206.5	291.9	54.1

Table 4 Heat flow data of compounds A–C

Compound	Process	$T_{\text{onset}}/^\circ\text{C}$	$T_{\text{end}}/^\circ\text{C}$	T_{peak}	$\Delta H/J\text{ g}^{-1}$
A	a	165.0	176.1	171.4	166.1 ± 4.3
	b	194.9	234.3	216.2	66.7 ± 2.2
	c	251.7	282.9	270.7	85.1 ± 3.8
B	a	79.5	87.4	82.6	5.2 ± 0.9
	b	103.3	114.1	106.2	97.8 ± 4.3
	c	225.1	302.4	277.2	-825.1 ± 5.7
C	a	88.5	94.5	90.83	10.7 ± 0.7
	b	97.4	111.2	103.0	91.2 ± 4.6
	c	217.7	302.1	272.7	-849.9 ± 18.8

for providing the kinetic parameters of the degradation process (FR, FWO and modified NPK kinetic methods).

In the thermogravimetric study, similar behaviour for all samples was found. Samples B and C show one highly exothermic decomposition stage in the range of 150–300 °C.

Kinetic study

The kinetic analysis was performed using the TG data in air for the substance’s decomposition at five heating rates: 5, 7, 10, 12 and 15 °C min⁻¹. To perform the kinetic analysis of the TG experimental data, three isoconversional methods were used, a differential one and two integral ones, respectively; fourth method elaborated by Sempere et al. [31, 32] and modified and developed by Vlase et al. [33, 34], the nonparametric kinetics method (NPK), in order to obtain kinetic parameters.

It is generally accepted that the reaction rate can be expressed as a product of two separable functions, $k(T)$ dependent only on the reaction temperature T and $f(\alpha)$ dependent on the reaction degree α , i.e.:

$$d\alpha/dt = k(T) \cdot f(\alpha) \tag{2}$$

where t is the reaction time. Under non-isothermal condition usually the reaction temperature depends linearly on time, $T = T_i + \beta t$, where β is the constant heating rate, so Eq. (1) becomes:

$$\beta \cdot d\alpha/dT = k(T) \cdot f(\alpha) \tag{3}$$

Equation (3) is the starting point for all the data processing methods used in kinetic analysis. The TG/DTG curves furnish directly the $d\alpha/dT$, α and T for different conversion degrees determined.

We used four different kinetic methods:

- Differential isoconversional by Friedman [35] (FR)

$$\ln(\beta \cdot d\alpha/dT)_\alpha = \ln[A \cdot f(\alpha)]_\alpha - E/RT \tag{4}$$

- Integral isoconversional by Flynn–Wall [36] and Ozawa [37] (FWO)

$$\ln \beta = \ln A/[R \cdot g(\alpha)] - 5.331 - 1.052 \cdot E/R \cdot T \tag{5}$$

where $g(\alpha) = \int_0^\alpha [d\alpha/f(\alpha)]$ is the integral form of the conversion function.

- The Kissinger–Akahira–Sunose [38, 39] method (KAS) with Eq (6):

$$\ln(\beta/T^2) = \ln[A \cdot R/E \cdot g(\alpha)] - E/R \cdot T \tag{6}$$

By these three methods, the plotting of the left member of Eqs. (4), (5) and (6) versus $1/T$, the value of the activation energy will be obtained from the line slope. The $f(\alpha)$ remain implicit, so these methods are “model free”.

By plotting the values of the activation energy E versus the conversion degree, the diagrams in Fig. 3 were obtained. Variations of E versus α exceed 10%, and these variations are non-monotonous. Therefore, a mean value of the activation energy is reasonable only for comparison (see Table 6).

- The modified NPK method [40–48]

According to Eq. (3), the experimental data are plotted in a 3D coordinate system ($d\alpha/dT$, T , α) and then interpolated for obtaining the reaction rate surface. This surface is partitioned as a $\mathbf{i} \times \mathbf{j}$ matrix \mathbf{M} .

$$\mathbf{M} = \{m_{ij}\} = \{f(T_i) \cdot g(\alpha_j)\} \tag{7}$$

The NPK method uses the singular value decomposition (SVD) algorithm to decompose matrix \mathbf{M} into two vectors [49]. The matrix \mathbf{M} is decomposed as follows:

$$\mathbf{M} = \mathbf{U}(\text{diag } \mathbf{s})\mathbf{V}^T \tag{8}$$

and the first columns of \mathbf{U} and \mathbf{V} matrix, respectively, \mathbf{u}_1 and \mathbf{v}_1 are analysed for determining the kinetic model, i.e.:

$$\mathbf{u}_1 = g(\alpha) \tag{9}$$

and a temperature dependence, i.e.:

$$\mathbf{v}_1 = f(T) \tag{10}$$

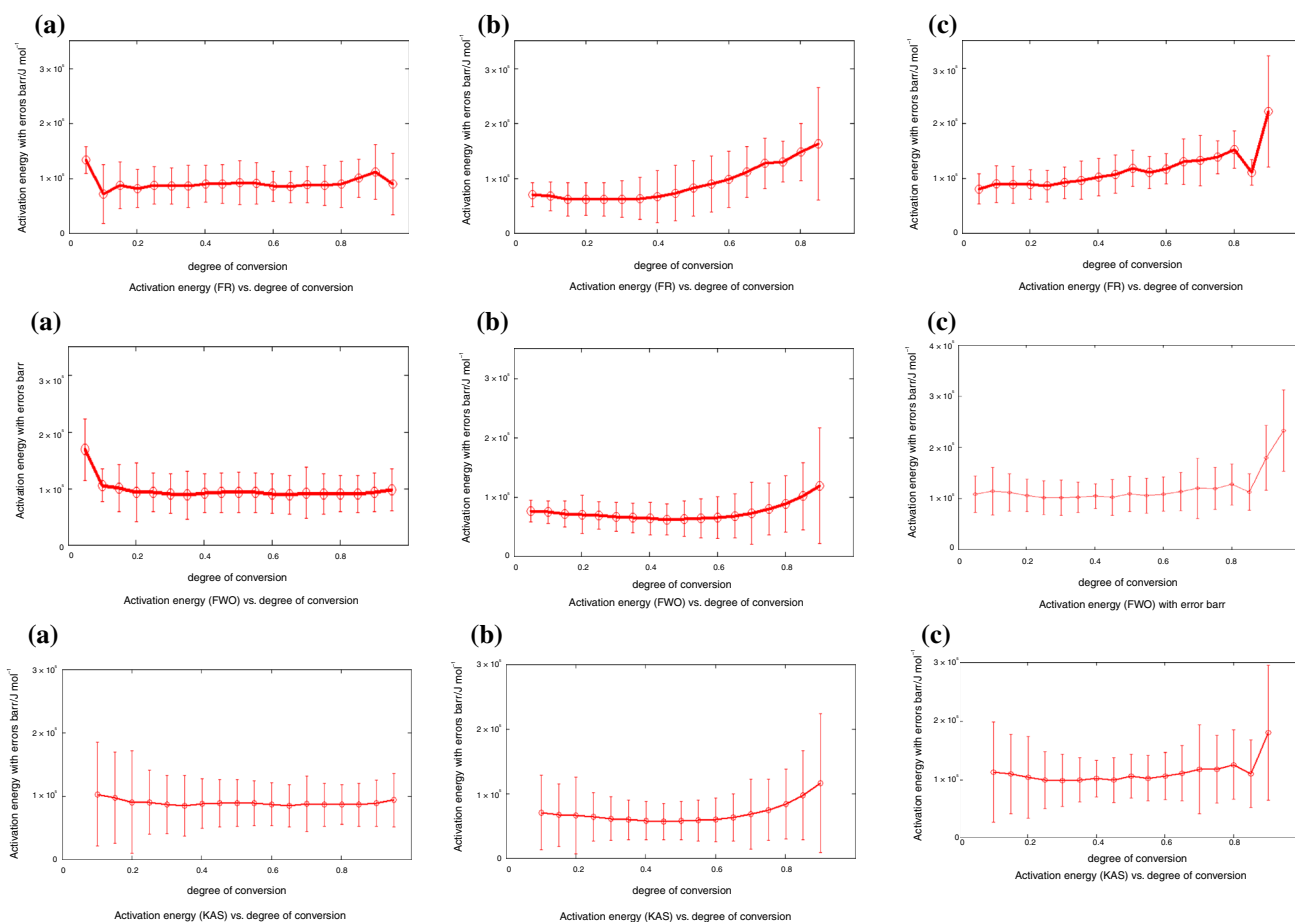


Fig. 3 Activation energy with errors bar versus conversion degree, determined by three different isoconversional methods for compounds A–C

Table 5 Mean activation energy according to modified NPK method

Compound	Process	$\lambda/\%$	A/s^{-1}	$E/kJ\ mol^{-1}$	n	m	Corr.	$\bar{E}/kJ\ mol^{-1}$
A	Main	78.7	3.35×10^{10}	92.1 ± 15.1	1	–	0.996	91.6 ± 20.5
	Secondary a	18.8	1.47×10^9	86.6 ± 5.1	–	1	0.996	
	Secondary b	2.4	5.69×10^{13}	113.8 ± 0.2	1	1	0.997	
B	Main	75.2	4.47×10^9	73.1 ± 11.1	1	–	0.994	73.1 ± 17.1
	Secondary a	24.5	1.03×10^9	73.1 ± 6.0	–	1	0.993	
C	Main	86.1	1.31×10^{12}	112.4 ± 19.8	1	–	0.998	111.3 ± 26.8
	Secondary a	11.8	2.66×10^{10}	106.4 ± 6.2	–	1	1	
		2.2	1.19×10^{10}	93.3 ± 0.8	1	1	0.999	

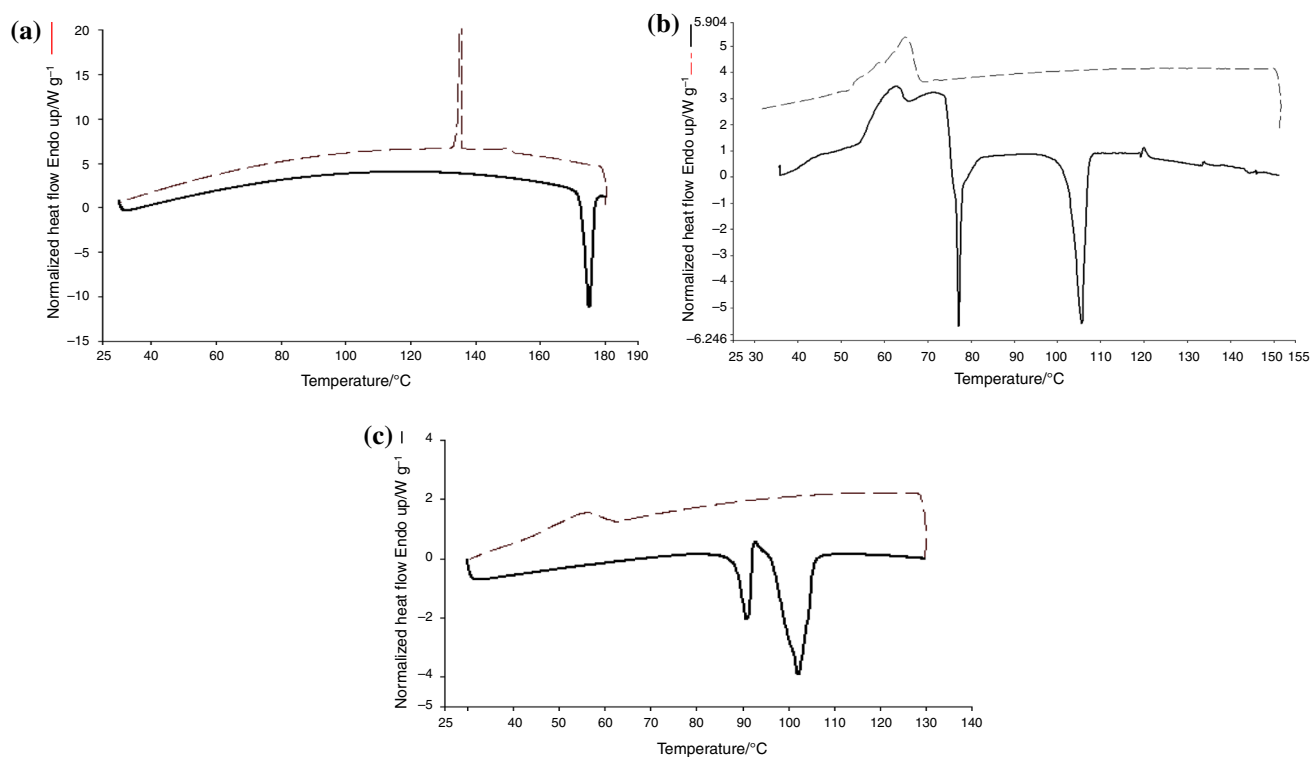
For the temperature dependence, the Arrhenius equation is selected, whereas for the kinetic model, we suggest the use of Šestak–Berggren equation [50]:

$$g(\alpha) = \alpha^m (1 - \alpha)^n \quad (11)$$

where α^m describes the influence of physical phenomenon related with the presence of reaction product and $(1 - \alpha)^n$ describes the chemical phenomenon which involves the remainder reactant $(1 - \alpha)$.

Table 6 Mean activation energy (\bar{E} /kJ mol⁻¹) determined by the four different kinetic analysis methods

Sample	Method			
	FR	FWO	KAS	NPK
A	91.4 ± 5.1	97.3 ± 6.9	94.0 ± 6.7	91.6 ± 20.5
B	90.7 ± 15.0	77.5 ± 7.3	72.9 ± 7.6	73.1 ± 17.2
C	114.4 ± 12.9	120.2 ± 12.6	111.4 ± 13.1	113.0 ± 27.2

**Fig. 4** DSC curves showing different situations at heating solid line, respectively, at cooling dashed line for A–C alkanolammonium salts

If the decomposition process is a result of two or more simultaneous steps, it means that $r = \sum r_i$ and consequently the matrix M becomes:

$$M = \sum M_i \quad (12)$$

The contribution of each step to the observed process is expressed by its variance, λ , so that $\sum \lambda_i = 100\%$. By the data processing with the NPK method, kinetic parameters were obtained (Table 5).

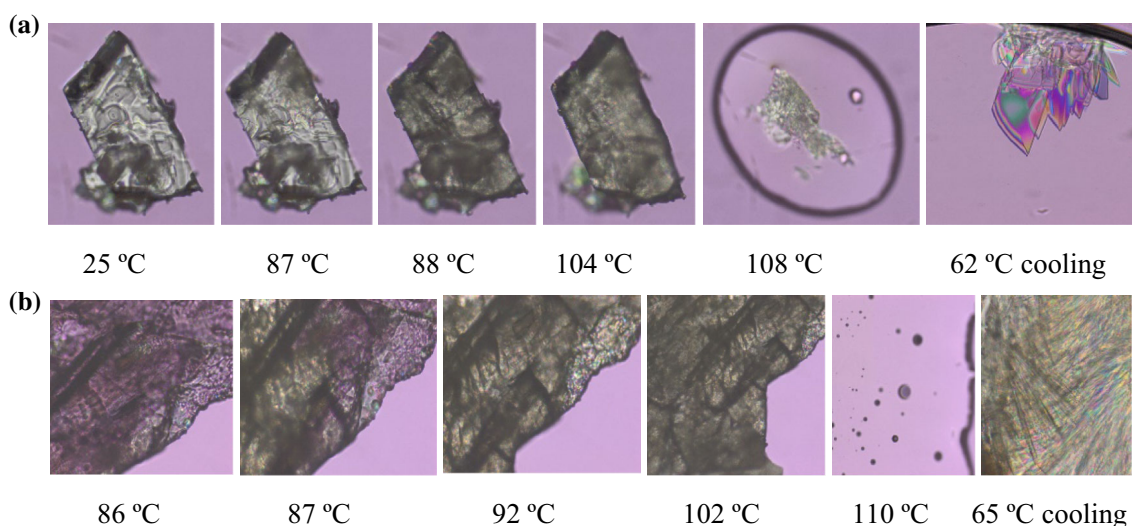
Activation energy value, presented in Table 6, indicates a reasonable agreement between the E values obtained by four different kinetic methods. The advantages of the NPK methods are: no supplementary approximations necessary for solving the temperature, and the respective conversion integrals and the kinetic description were complete.

Calorimetric analysis of compounds A–C

DSC curves and melting characteristics of A–C compounds under N₂ atmosphere are illustrated in Fig. 4 and Table 7. DSC curves of compounds A are characterized by the presence of one endotherm peak associated with melting with decomposition and the absence of solvate forms (Fig. 4), while for compounds B and C, a phase transition crystal–crystal was observed before the endotherm peak associated with melting. The transition between different phases was examined under Olympus BX53M polarizing microscope (POM) equipped with Linkam hot stage (Fig. 5).

Table 7 DSC characteristics of compounds A–C

Compound	Heating					Cooling				
	Process	$T_{\text{onset}}/^{\circ}\text{C}$	$T_{\text{end}}/^{\circ}\text{C}$	T_{peak}	$\Delta H/J \text{ g}^{-1}$	Process	$T_{\text{onset}}/^{\circ}\text{C}$	$T_{\text{end}}/^{\circ}\text{C}$	T_{peak}	$\Delta H/J \text{ g}^{-1}$
A	a	172.44	176.77	175.02	– 207.03	a	135.77	134.49	135.51	134.24
B	a	54.83	65.14	61.66	44.66	a	67.95	52.23	64.66	84.78
	b	76.15	78.07	77.18	– 100.20					
	c	102.80	107.23	105.54	– 120.45					
C	a	88.23	92.33	90.95	– 44.44	a	61.79	44.19	56.15	29.82
	b	97.64	105.62	102.17	– 140.00					

**Fig. 5** Optical micrographs of the crystalline solids B **a** and C **b** showing the transitions between different phases taken with filter $\lambda = 530 \text{ nm}$

Conclusions

New alkanolammonium salts based on pharmaceutical acid 4-NBA have been synthesised, and their thermal behaviour were compared. The studied compounds display various phase transitions in the solid state, which have been examined by thermal analysis, differential scanning calorimetry and hot-stage microscopy. Since in this study the 4-nitrobenzoate anion is a constant, differences of the solid state can be attributed to the alkyl and hydroxyl groups of the cation. When the cation possesses only one hydroxyl group (4-NBA MEA), the salt shows one endotherm peak associated with melting and decomposition. Substitution of H atoms linked to N atom in alkanolamines, with hydroxyl and ethyl groups, leads to different hydrogen-bonding network in final compounds and exhibits a phase transition crystal–crystal below the melting point. Compounds B and C show low melting points near 100 °C, compared to compound A which melts at 175 °C. The activation energies of the decomposition reactions were

determined using four different methods, the values obtained by KAS and NPK being in good agreement. Kinetic results showed differences in activation energy between the studied compounds which increased in the order of $C > A > B$.

Acknowledgements Authors thank the bilateral Moldova-Romanian project 16.80013.5007.04/Ro and the Romanian National Authority for Scientific Research and Innovation, CCCDI-UEFISCDI, project PN3-P3-217/24 BM/19.09.2016

References

1. Ono N. The nitro group in organic synthesis. New York: Wiley; 2002.
2. Zaragoza Dörwald F. Nitro compounds. Weinheim: Wiley-VCH Verlag GmbH & Co. KgaA; 2012.
3. Zollinger H. Color chemistry. New York: VCH Publishers; 1987.
4. Gasiewicz TA. Nitro compounds and related phenolic pesticides. In: Hayes WR, Laws ER, editors. Handbook of pesticide toxicology. Cambridge: Academic Press Inc.; 1991. p. 1191–270.

- Straus MJ. The nitroaromatic group in drug design. Pharmacology and toxicology (for nonpharmacologists). *Ind Eng Chem Prod Res Dev.* 1979;18:158–66.
- Walsh JS, Miwa GT. Bioactivation of drugs: risk and drug design. *Annu Rev Pharmacol Toxicol.* 2011;51:145–67.
- Truong DD. Tolcapone: review of its pharmacology and use as adjunctive therapy in patients with Parkinson's disease. *Clin Interv Aging.* 2009;4:109–13.
- Sorkin EM, Clissold SP, Brogden RN. Nifedipine. A review of its pharmacodynamic and pharmacokinetic properties, and therapeutic efficacy, in ischaemic heart disease, hypertension and related cardiovascular disorders. *Drugs.* 1985;30:182–274.
- Mattila MAK, Larni HM. Flunitrazepam: a review of its pharmacological properties and therapeutic use. *Drugs.* 1980;20:353–74.
- Agarwal A, Dhole TN, Sharma YK. Evaluation of p-nitro benzoic acid (pnb) inhibition test to differentiate Mycobacterium tuberculosis complex from non-tuberculous mycobacteria using microscopic observation of drug susceptibility (MODS) methodology. *Indian J Tuberc.* 2014;61:232–5.
- Shakoor S, Ahsan T, Jabeen K, Raza M, Hasan R. Use of p-nitrobenzoic acid in 7H10 agar for identification of *Mycobacterium tuberculosis* complex: a field study. *Int J Tuberc Lung Dis.* 2010;14:1644–6.
- Dinesh Kumar G, Amirthaganesan G, Sethuram M. Synthesis, spectral, structural, thermal and optical studies on dimethylammonium 4-nitrobenzoate—an organic charge transfer complex. *Optik.* 2016;127:336–40.
- Arumanayagam T, Murugakoothan P. Growth, linear and non-linear optical studies on guanidinium 4-nitrobenzoate (GuNB): an organic NLO material. *Optik.* 2012;123:1153–6.
- Sasikala V, Sajjan D, Job Sabu K, Arumanayagam T, Murugakoothan P. Electronic structure, vibrational spectral and intervening orbital interactions studies of NLO material: guanidinium 4-nitrobenzoate. *Spectrochim Acta A Mol Biomol Spectrosc.* 2015;139:555–72.
- Selvakumar E, Anandha babu G, Ramasamy P, Rajnikant, Murugesan V, Chandramohan A. Synthesis, growth and spectroscopic investigation of an organic molecular charge transfer crystal: 8-hydroxy quinolinium 4-nitrobenzoate 4-nitrobenzoic acid. *Spectrochim Acta A Mol Biomol Spectrosc.* 2014;117:259–63.
- Hernández-Paredes J, Terán-Reprieto ME, Esparza-Ponce HE, Sotelo-Mundo RR, Hernández-Negrete O, Reyes-Márquez V, Álvarez-Ramos ME. Growth and characterization of L-histidinium-4-nitrobenzoate (1:1) multi-component molecular complex. *J Mol Struct.* 2015;1102:323–30.
- Shkir M, AlFaify S, Abbas H, Muhammad S. First principal studies of spectroscopic (IR and Raman, UV–visible), molecular structure, linear and nonlinear optical properties of L-arginine p-nitrobenzoate monohydrate (LANB): a new non-centrosymmetric material. *Spectrochim Acta A Mol Biomol Spectrosc.* 2015;147:84–92.
- Kavitha CN, Kaur M, Anderson BJ, Jasinski JP, Yathirajan HS. 1-Piperonylpiperazinium 4-nitrobenzoate monohydrate. *Acta Crystallogr Sect E: Struct Rep Online.* 2014;70:o270–1.
- Balasubramani K, Fun H-K. 2,3-Diamino-pyridinium 4-nitrobenzoate. *Acta Crystallogr Sect E: Struct Rep Online.* 2009;65:o1511–2.
- Srinivasan BR, Sawant JV, Raghavaiah P. Synthesis, spectroscopy, thermal studies and supramolecular structures of two new alkali-earth 4-nitrobenzoate complexes containing coordinated imidazole. *J Chem Sci.* 2007;119:11–20.
- Chumakov Y, Simonov Y, Grozav M, Crisan M, Bocelli G, Yakovenko A, Lyubetsky D. Hydrogen-bonding network in the organic salts of 4-nitrobenzoic acid. *Cent Eur J Chem.* 2006;4:458–75.
- Crisan M, Bourosh P, Chumakov Y, Petric M, Iliia G. Supramolecular assembly and ab initio quantum chemical calculations of 2-hydroxyethylammonium salts of para-substituted benzoic acids. *Cryst Growth Des.* 2013;13:143–54.
- Chicu SA, Grozav M, Kurunczi L, Crisan M. SAR for amine salts of carboxylic acids to *Hydractinia echinata*. *Rev Chim.* 2008;59:582–7.
- Crisan ME, Bourosh P, Maffei ME, Forni A, Pieraccini S, Sironi M, Chumakov YM. Synthesis, crystal structure and biological activity of 2-hydroxyethylammonium salt of p-aminobenzoic acid. *PLoS ONE.* 2014;9:e101892.
- Crisan M, Grozav M, Kurunczi L, Iliia G, Bertea C. Inhibitory effects of some synthetic monoethanolaminesalts of para-substituted benzoic acids and corresponding benzoic acids on cucumber seed germination. *J Plant Interact.* 2007;2:53–61.
- Crisan M, Grozav M, Bertea C. *Arabidopsis thaliana* seed germination and early seedling growth are inhibited by monoethanolamine salts of parahalogenated benzoic acids. *J Plant Interact.* 2009;4:271–7.
- Cruz-Cabeza AJ. Acid–base crystalline complexes and the pK_a rule. *CrystEngComm.* 2012;4:6362–5.
- PubChem Compound Database <https://www.ncbi.nlm.nih.gov/pccompound>.
- Silverstein RM, Webster FX. Spectrometric identification of organic compounds. 6th ed. New York: Wiley; 1998.
- Pavia DL, Lampman GM, Kriz GS, Vyvyan JR. Introduction to spectroscopy. Boston: Cengage Learning, Brooks/Cole; 2009.
- Serra R, Nomen R, Sempere J. The non-parametric kinetics. A new method for the kinetic study of thermoanalytical data. *J Therm Anal Calorim.* 1998;52:933–43.
- Serra R, Sempere J, Nomen R. A new method for the kinetic study of thermoanalytical data: the non-parametric kinetics method. *Thermochim Acta.* 1998;316:37–45.
- Vlase T, Vlase G, Doca N, Bolcu C. Processing of non-isothermal TG data. Comparative kinetic analysis with NPK method. *J Therm Anal Calorim.* 2005;80:59–64.
- Vlase T, Vlase G, Doca N, Iliia G, Fulfias A. Coupled thermogravimetric-IR techniques and kinetic analysis by non-isothermal decomposition of Cd²⁺ and Co²⁺ vinyl-phosphonates. *J Therm Anal Calorim.* 2009;97:467–72.
- Friedman HL. Kinetics of thermal degradation of char-foaming plastics from thermogravimetry: application to a phenolic resin. *J Polym Sci.* 1965;6C:183–95.
- Flynn JH, Wall LA. A quick, direct method for the determination of activation energy from thermogravimetric data. *Polym Lett.* 1966;4:323–8.
- Ozawa T. A new method of analysing thermogravimetric data. *Bull Chem Soc Jpn.* 1965;38:1881–6.
- Akahira T, Sunose T. Joint convention of four electrical institutes. Research report Chiba Institute of Technology. *Sci Technol.* 1971;16:22–31.
- Kissinger HE. Reaction kinetics in differential thermal analysis. *Anal Chem.* 1957;29:1702–6.
- Birta N, Doca N, Vlase G, Vlase T. Kinetic of sorbitol decomposition under non-isothermal conditions. *J Therm Anal Calorim.* 2008;92:35–638.
- Anghel M, Vlase G, Bilanin M, Vlase T, Albu P, Fulfias A, Tolan I, Doca N. Comparative study on the thermal behavior of two similar triterpenes from birch. *J Therm Anal Calorim.* 2013;113:1379–85.
- Ledeti I, Vlase G, Vlase T, Bercean V, Fulfias A. Kinetic of solid state degradation of transitional coordinative compounds containing functionalized 1,2,4 -triazolic ligand. *J Therm Anal Calorim.* 2015;121(3):1049–57.

43. Patrutescu C, Vlase G, Turcus V, Ardelean D, Vlase T, Albu P. TG/DTG/DTA data used for determining the kinetic parameters of the thermal degradation process of an immunosuppressive agent: mycophenolate mofetil. *J Therm Anal Calorim.* 2015;121(3):983–8.
44. Ledeti I, Vlase G, Vlase T, Fuliş A, Şuta LM. Comparative thermal stability of two similar-structure hypolipidemic agents—Simvastatin and Lovastatin—kinetic study. *J Therm Anal Calorim.* 2016;125:769–75.
45. Ledeti I, Bercean V, Vlase G, Vlase T, Ledeti A, Şuta L. Betulonic acid. Study of thermal degradation by kinetic approach. *J Therm Anal Calorim.* 2016;125:785–91.
46. Fuliş A, Ledeti I, Vlase G, Vlase T, Şoica C, Dehelean C, Oprean C, Bojin F, Şuta M, Bercean V, Avram S. Thermal degradation, kinetic analysis, and apoptosis induction in human melanoma for oleanolic and ursolic acids. *J Therm Anal Calorim.* 2016;125:759–68.
47. Vlase G, Modra D, Albu P, Ceban I, Bolcu C, Vlase T. Thermal behavior of saturated phthalic-type polyesters. Influence of the branching polyol. *J Therm Anal Calorim.* 2017;127:409–14.
48. Albu P, Doca SC, Anghel A, Vlase G, Vlase T. Thermal behavior of sodium alendronate. A kinetic study under non-isothermal conditions. *J Therm Anal Calorim.* 2017;127:571–6.
49. Wall ME. Singular value decomposition and principal component analysis. In: Berrar DP, Dubitzky W, Granzow M, editors. *A practical approach to microarray data analysis.* Dordrecht: Kluwer; 2003. p. 91–109.
50. Šestak J, Berggren G. Study of the kinetics of the mechanism of solid-state reactions at increasing temperatures. *Thermochim Acta.* 1971;3:1–12.